
A Refined Method for Quantification of Myocardial Oxygen Consumption Rate Using Mean Transit Time with Carbon-11-Acetate and Dynamic PET

Yong Choi, Sung-Cheng Huang, Randall A. Hawkins, Carl K. Hoh, Janine Krivokapich, Denis B. Buxton, Jürgen J. Armbrecht, Karl T. Sun, Michael E. Phelps and Heinrich R. Schelbert

Division of Nuclear Medicine and Biophysics, Department of Molecular and Medical Pharmacology, Laboratory of Nuclear Medicine (DOE), Laboratory of Structural Biology and Molecular Medicine; The Crump Institute for Biological Imaging; Division of Cardiology, Department of Medicine, School of Medicine, University of California, Los Angeles, California*

The utility of the mean transit time equation was investigated for estimation of the myocardial clearance rate constant of ^{11}C -acetate, which is proportional to myocardial oxygen consumption rates. The mean transit time approach was also employed to generate parametric images of the clearance rate constant of ^{11}C -acetate with dynamic PET imaging in 20 normal human studies. Input function delays and cutoff errors due to the truncation of the myocardial tissue time-activity curve at a finite time were corrected. The clearance rate constants estimated by mean transit time correlated well with the estimates by conventional monoexponential fitting (15 min (truncation time): $Y = 0.01 + 0.94X$, correlation coefficient (r) = 0.99; 16 min: $Y = 0.03 + 0.94X$, $r = 0.98$; 20 min: $Y = 0.03 + 0.84X$, $r = 0.99$). The clearance rate constants estimated by the mean transit time approach also correlated well ($r = 0.94$) with the measured rate-pressure products. The quality and noise level of parametric images of the clearance rate constants generated by mean transit time are improved over those generated by monoexponential fitting. Additional advantages of the mean transit time approach compared to the standard monoexponential fitting method for estimating myocardial clearance rate constant of ^{11}C -acetate include ease of input function delay correction, less sensitivity to the shape of the input function and elimination of subjective data selection of the linear portion of the clearance data on a semilog plot. Thus, this approach is expected to facilitate objective quantitative analysis of indices of myocardial oxygen consumption.

J Nucl Med 1993; 34:2038–2043

Received Mar. 18, 1993; revision accepted Jul. 18, 1993.

For correspondence and reprints contact: Yong Choi, PhD, PET Facility B-938, Dept. of Radiology, University of Pittsburgh Medical Center, DeSoto at O'Hara Streets, Pittsburgh, PA 15213-2582.

*Operated for the U.S. Department of Energy by the University of California under contract #DE-FC03-87ER60615.

Carbon-11-acetate is avidly extracted from the plasma by myocardial tissue and accumulates in myocardium approximately in proportion to myocardial blood flow (I). Once ^{11}C -acetate is transported into the mitochondrion of a cell, it is rapidly converted into ^{11}C -acetylcoenzyme-A (acetyl-CoA) by acetyl-CoA synthetase. Carbon-11-acetyl-CoA then enters the tricarboxylic acid (TCA) cycle, and equilibrates rapidly with the glutamate and aspartate pools via transamination reactions. The ^{11}C label is released as ^{11}C CO_2 at a rate proportional to the oxidation rate of the TCA cycle (2,3). Studies in animal models have shown that the early portion of the ^{11}C clearance is monoexponential and that the clearance rate, k_{mono} , of this phase is proportional to the TCA cycle flux (4–9). The clearance rate constant, k_{mono} , correlated well with independently measured rates of myocardial oxygen consumption (MVO_2) in animal studies (4–9) and with the rate pressure product in humans (10,11). Additionally, because of the computational simplicity of monoexponential fitting, generation of parametric images or polar maps of k_{mono} is possible (12,13).

Although the monoexponential fitting approach is computationally simple and provides reasonably reliable numerical indices of myocardial oxygen consumption, the numerical accuracy of the estimates can be affected by the shape of the input function and by the selection of the data points on the tissue time-activity curve for analysis. In addition, pixel-by-pixel parametric images of k_{mono} are noisy and require heavy smoothing of the original dynamic image data. More rigorous compartment modeling approaches have also been developed to obtain more accurate estimates of myocardial oxygen consumption rates (2,14). However, these modeling approaches remain to be validated. Further, they are difficult to apply clinically because of their computational and technical complexity.

The purpose of this study was to develop and investigate a method to estimate rates of myocardial oxygen consumption.

tion, reflected by the clearance rate constant, using the mean transit time equation defined from statistical moment theory (15–18). This approach is expected to be more accurate, less noise sensitive than conventional monoexponential fitting approaches and is computationally much simpler than the compartmental modeling approaches.

MATERIALS AND METHODS

Study Population

Twenty baseline (resting) and intervention studies (five exercise and five dobutamine studies) were performed in 10 young healthy male volunteers, aged 18–31 yr (average 24 ± 5 yr). None of the volunteers had suspected or documented cardiac disease. The study protocol was approved by the UCLA Human Subject Protection Committee. Each participant gave written informed consent. PET studies included in this investigation have been reported in other studies (10,19).

Image Acquisition and Scan Protocol

Five normal subjects were studied at rest and during bicycle exercise with an ECAT III whole-body tomograph (20). The other five normals were studied at rest and during dobutamine infusion with a Siemens/CTI 931 tomograph (Siemens Medical Systems, Inc., Hoffman Estates, IL). Photon attenuation was corrected with transmission images obtained with a $^{68}\text{Ge}/^{68}\text{Ga}$ external ring source.

Image acquisition was initiated simultaneously with intravenous administration of about 10–15 mCi of $[1-^{11}\text{C}]$ -acetate given as a bolus over 30 sec. The image acquisition sequence consisted of six 30-sec, eight 60-sec, five 120-sec and seven 240-sec frames (ECAT III studies) or twelve 10-sec, eight 60-sec and three 120-sec frames (Siemens/CTI 931 studies).

Heart rates and systolic blood pressures were measured throughout the imaging period. Exercise studies in five normals were performed in the supine position with a bicycle ergometer. Work loads ranged from 25 to 130 W, with a mean \pm s.d. of 62 ± 43 W. In dobutamine intervention studies, dobutamine was infused continuously at a $40\text{-}\mu\text{g}/\text{kg}/\text{min}$ dose during 16 min of imaging to maintain a constant rate pressure product. The more detailed experimental procedures employed in normal human studies have been described elsewhere (10,19).

Image Analysis

Global myocardial tissue time-activity curves were generated from regions of interest (ROIs) of left ventricular myocardium at a single midventricular level of dynamic PET images in each study. The arterial blood radioactivity concentration in each study was derived from a ROI (about 60 mm^2 in size) assigned to the left ventricular blood pool also at a midventricular level (21–24). The myocardial tissue and blood-pool time-activity curves were decay-corrected. ROI definition of activity concentration measurements were facilitated by the Apple® Macintosh® image processing program Explorer™.

Calculation of the Clearance Rate Constant of the Tracer

The linear portion (on a semilog plot) of the initial phase of ^{11}C -acetate myocardial time-activity curve, $C_i(t)$, was fitted to a monoexponential function using an iterative least-squares method. The clearance rate constant of this phase is termed " k_{mono} ". The linear portion of the curve was identified visually from semilog plots of the myocardial time-activity curve.

The clearance rate constant of the initial linear portion of the myocardial tissue kinetic curve was also calculated using statistical moment theory for determination of mean transit time. This parameter was termed " k " and compared to the values, k_{mono} , estimated from monoexponential fitting. The mean transit time of a tracer with a time-course of activity concentration $C_i(t)$ in a system of interest is defined by the first moment and termed, \bar{t}_1 , as follows (15–18):

$$\bar{t}_1 = \frac{\int_0^{\infty} tC_i(t) dt}{\int_0^{\infty} C_i(t) dt} \quad \text{Eq. 1}$$

If the input function of the tracer to the system is delayed by \bar{t}_d , the mean transit time of the tracer in the system can be obtained by subtracting the delay time of the input due to the additive property of the first moment (15–18):

$$\bar{t} = \frac{\int_0^{\infty} tC_i(t) dt}{\int_0^{\infty} C_i(t) dt} - \frac{\int_0^{\infty} tC_b(t) dt}{\int_0^{\infty} C_b(t) dt} = \bar{t}_1 - \bar{t}_d, \quad \text{Eq. 2}$$

where $C_i(t)$ is ^{11}C radioactivity concentration in myocardial tissue and $C_b(t)$ is ^{11}C -acetate activity in arterial blood.

If the transit time distribution is a monoexponential function, Ae^{-kt} , where A is a constant, with input function delay, \bar{t}_d , the mean transit time of the tracer, \bar{t} , in myocardium can be expressed as:

$$\bar{t} = \bar{t}_1 - \bar{t}_d = \frac{1}{k}. \quad \text{Eq. 3}$$

Since ^{11}C -acetate in blood is quickly extracted and metabolized, the arterial ^{11}C radioactivity curve derived from the left ventricular blood-pool ROI was integrated up to 3 min to approximate the delay time of the input function.

If the first moment is calculated from a finite time course of myocardial tissue time-activity data from \bar{t}_d to $T + \bar{t}_d$, the cutoff error due to the truncation of the myocardial tissue time-activity curve at $T + \bar{t}_d$ can be estimated. The cutoff error containing mean transit time, \bar{t} , can be estimated by the following equation with the assumption of a bolus input function and a negligible transit time across capillary and cell membranes of ^{11}C -acetate:

$$\bar{t} = \frac{\int_{\bar{t}_d}^{T + \bar{t}_d} te^{-k(t - \bar{t}_d)} dt}{\int_{\bar{t}_d}^{T + \bar{t}_d} e^{-k(t - \bar{t}_d)} dt} - \bar{t}_d = \frac{\int_0^T (t + \bar{t}_d)e^{-kt} dt}{\int_0^T e^{-kt} dt} - \bar{t}_d. \quad \text{Eq. 4}$$

By solving the integration, Equation 4 yields:

$$\bar{t} = \bar{t}_1 - \frac{Te^{-kT}}{1 - e^{-kT}} - \bar{t}_d = \bar{t} - \frac{Te^{-kT}}{1 - e^{-kT}} = \frac{1}{k} - \frac{Te^{-kT}}{1 - e^{-kT}}. \quad \text{Eq. 5}$$

The term, $Te^{-kT}/1 - e^{-kT}$, of Equation 5 is caused by the truncation of the myocardial tissue time-activity curve at $T + \bar{t}_d$. The

TABLE 1
Hemodynamic Parameters

Conditions	Heart rate (min ⁻¹)	Systolic blood pressure (mmHg)	RPP (mmHg/min)
Baseline (n = 10)	64 ± 9	110 ± 5	7034 ± 998
Exercise (n = 5)	112 ± 17*	153 ± 18*	17362 ± 4585*
Dobutamine (n = 5)	118 ± 26*	177 ± 18*	20685 ± 4206*

*p < 0.001 compared to baseline studies.
RPP = rate pressure product.

relationship between \bar{t} and k of Equation 5 was found to be monotonic in all studies for time \bar{t}_d to $T + \bar{t}_d$. Therefore, by estimating \bar{t} using Equation 4, k values can be obtained using Equation 5. Since there is no analytical equation for k as a function of \bar{t} (Equation 5), k values were obtained with a look-up table generated using Equation 5. Different values of $T + \bar{t}_d$ (15, 16 and 20 min) were used to examine the effect of the selection of a value T on the estimated k values.

In addition to regional analysis using the time-activity curves generated from myocardial ROIs, parametric images of the rate constant, k , were generated by applying Equations 4 and 5 to each image pixel. For the parametric imaging approach, background noise and blood-pool region were masked by applying a threshold value of 0.6 of the maximum pixel value on the myocardial activity image. The myocardial activity image was obtained by summing images recorded between 3 and 16 or 20 min after tracer injection, when blood-pool activity was relatively low compared to myocardial activity. Spillover of activity from the left ventricular blood pool into myocardium on the parametric image was corrected as follows: (1) obtain blood-pool image by summing the initial 2-min images and normalize it so that the maximum pixel value = 1; (2) mask out myocardial tissue region on the blood-pool image using the myocardial activity image obtained above; (3) smooth the masked blood-pool image using a Gaussian kernel so that the boundaries of left ventricular blood pool and myocardial tissue correspond to the image resolution of the employed image reconstruction filter; and (4) subtract the smoothed blood-pool image, multiplied by the left ventricular time-activity curves, from the original dynamic images.

The effect of spillover of activity from left ventricular blood pool to myocardial tissue was further examined with computer

simulation using a constant spillover fraction of 0.15. The clearance rate constants, k_{mono} and k were calculated with and without spillover correction for myocardial tissue time-activity curves using both monoexponential fitting and the mean transit time equation in order to examine the effect of the spillover correction.

RESULTS

Hemodynamic parameters for the 20 studies are summarized in Table 1. Exercise and dobutamine interventions significantly increased heart rate, systolic blood pressure and the rate pressure product compared to the baseline studies.

Carbon-11-acetate time-activity curves of left ventricular blood pool and myocardial tissue are illustrated in Figure 1. As seen, ¹¹C activity in arterial blood clears quickly during the first few minutes after the tracer injection, reflecting high extraction fraction of ¹¹C-acetate. Thereafter, it decreases more slowly due to the production of ¹¹C-CO₂ by oxidation of ¹¹C-acetate.

Resting and stress myocardial tissue time-activity curves from one normal volunteer are also illustrated in Figure 1. The curves are characterized by an initial rapid uptake of ¹¹C-acetate which is related to blood flow, with a subsequent biexponential clearance. The myocardial time-activity curves obtained from the exercise studies demonstrate an increased clearance rate of ¹¹C activity from myocardium, which is consistent with increased TCA cycle activity during exercise. The early linear clearance phase of the tissue curve, as indicated by the arrows in Figure 1, was fitted to a monoexponential function in order to derive k_{mono} .

Input function delay times calculated using the second term of Equation 2 for 20 studies revealed consistent estimates of \bar{t}_d and ranged from 1.03 to 1.57 min with average ± s.d. of 1.25 ± 0.13 min.

Values for k_{mono} estimated by monoexponential fitting and for k estimated by the mean transit time equation without correction for the spillover of activity from blood pool to myocardial tissue are compared in Figure 2. The estimates obtained by the two different methods showed an excellent correlation over a wide range of k_{mono} values. In

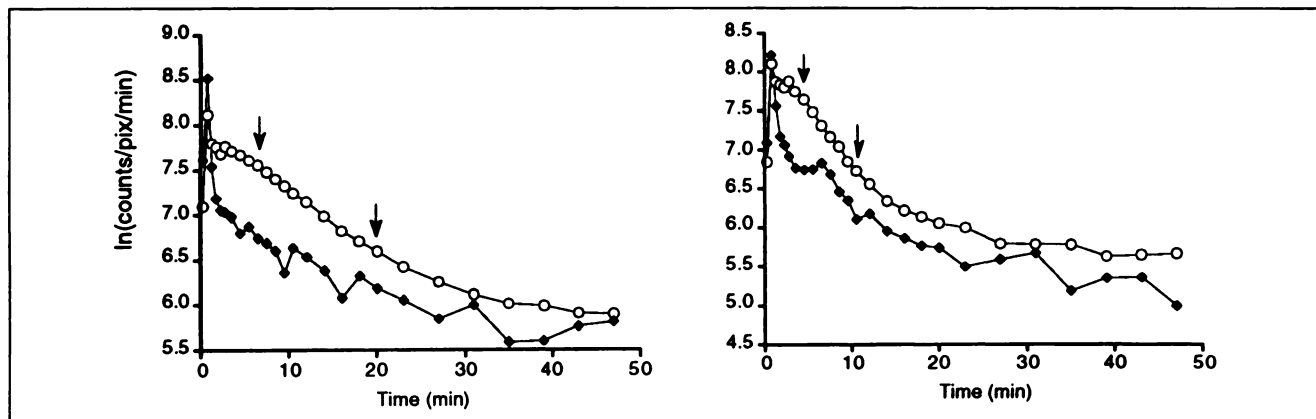


FIGURE 1. Time-activity curves of left ventricular blood pool (solid diamonds) and myocardial tissue (open circles) in a baseline (left) and in an exercise study (right) obtained from a normal volunteer study. Arrows indicate start points and end points for monoexponential fitting.

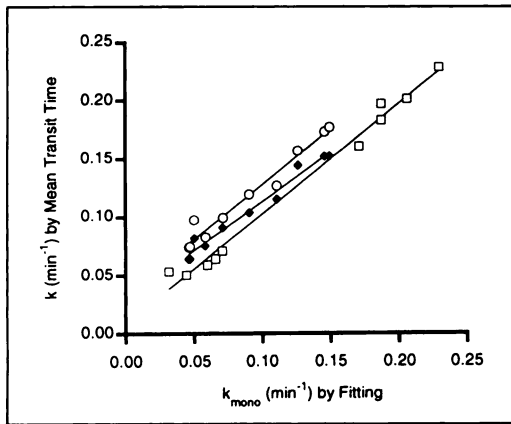


FIGURE 2. Comparison of k_{mono} (min^{-1}) values estimated by monoexponential fitting and k values by mean transit time equation using $T + \bar{t}_d = 15$ (open squares), 16 (open circles) and 20 min (solid diamonds). Solid lines are linear regressions to the data and revealed $Y = 0.01 + 0.94X$, correlation coefficient (r) = 0.99, $Y = 0.03 + 0.94X$, $r = 0.98$ and $Y = 0.03 + 0.84X$, $r = 0.99$ for $T + \bar{t}_d = 15, 16$ and 20 min, respectively.

addition, the estimates, k , obtained by the mean transit time equation were relatively insensitive to the truncation time, $T + \bar{t}_d$. As expected, k values obtained by regional analysis correlated well with k values obtained by the parametric imaging approach ($r = 0.99$, $n = 10$).

The correlations between the rate pressure product and the values for k_{mono} and those for k for the 20 studies are illustrated in Figure 3. Consistent with previous reports, the clearance rate constants of the early phase of the myocardial tissue time-activity curves estimated by the monoexponential curve fitting correlated well (correlation coefficient, $r = 0.90$) with the rate pressure product, which is an indirect indicator of myocardial oxygen consumption. The k values obtained using the mean transit time equation also correlated well ($r = 0.94$) to the rate pressure products.

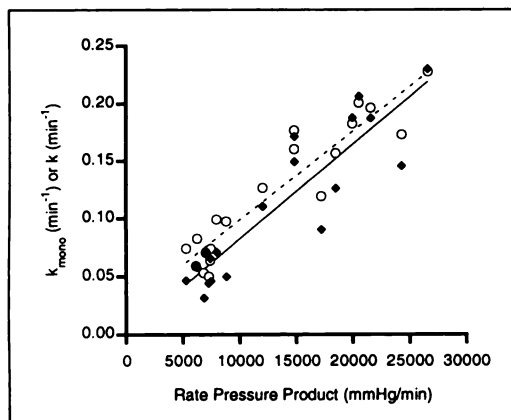


FIGURE 3. Correlations between rate pressure product (mmHg/min) and k_{mono} (min^{-1}) values estimated by monoexponential curve fitting (solid diamonds) and k values estimated by mean transit time equation using truncation time, $T + \bar{t}_d = 15$ or 16 min (open circles) in 20 studies. Solid and dashed lines are linear regression line to the data obtained by the curve fitting and by mean transit time equation respectively, and revealed $Y = 8.21 \times 10^{-6}X$, $r = 0.90$ and $Y = 0.02 + 7.71 \times 10^{-6}X$, $r = 0.94$, respectively.

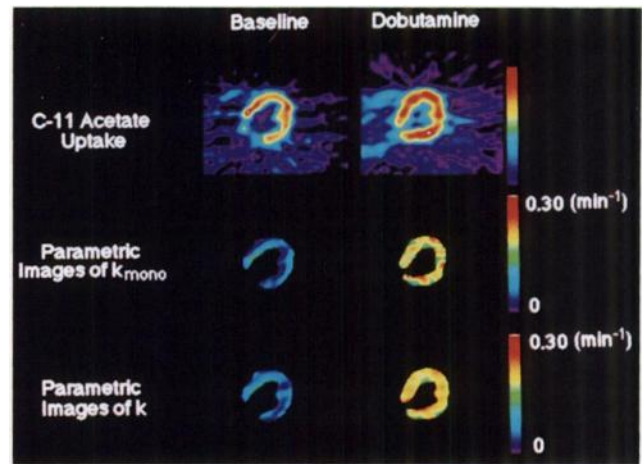


FIGURE 4. (Upper panel) Carbon-11-acetate images of baseline (left) and dobutamine intervention (right) studies recorded at 5 and 3.5 min after the tracer injection, respectively. (Middle panel) Parametric images of k_{mono} generated by monoexponential fitting. (Lower panel) Parametric images of k values generated by mean transit time equation. Parametric images of k_{mono} and k values are scaled to units of min^{-1} .

Figure 4 illustrates images of ^{11}C -acetate uptake and parametric images of k_{mono} and k values generated by monoexponential fitting and by the mean transit time equation, respectively, to each image pixel for a normal study. The noise level of parametric images generated by the mean transit time equation was significantly lower ($p < 0.01$) than that by monoexponential fitting. The percent s.d. of ROI values on parametric images generated by monoexponential fitting and by the mean transit time equation were $29\% \pm 14\%$ and $17\% \pm 10\%$ (mean \pm s.d., $n = 10$), respectively. Computational time for generating parametric images using monoexponential fitting and using the mean transit time equation was comparable, about 20 sec per image (128×128 pixels) using the BLD (Digital Equipment Corp., Maynard, MA) (25) and VAX 4000 (Digital Equipment Corp., Maynard, MA) for both approaches.

The effect of spillover of activity on the calculated k_{mono} and k values was different for the estimates obtained by the two different approaches. The spillover correction revealed that the ratio of k_{mono} values without spillover correction to those with the correction was 0.97 ± 0.03 ($n = 11$) in the monoexponential fitting approach and that the ratios of the k values were 1.05 ± 0.05 ($n = 11$) and 1.03 ± 0.04 ($n = 11$) by the mean transit time equation using $T + \bar{t}_d$ of 16 and 20 min respectively.

DISCUSSION

This study indicates that estimating the clearance rate constant of ^{11}C -acetate from myocardium based on mean transit time in tissue is practical. The method generates values comparable to those estimated with standard monoexponential fitting of the early clearance phase. The method can be used to estimate an index of myocardial oxygen consumption.

This approach has several advantages over the conventional exponential fitting approach for dynamic ^{11}C -acetate

studies. When monoexponential curve fitting is used, visual inspection of the shape of the myocardial tissue time-activity curve is required to identify the linear portion of the curve on a semilog plot. This requires an additional step in data processing and, more importantly, could be vulnerable to inter-observer and intra-observer variability in selecting the linear portion of the plot. Estimates based on the mean transit time equation, however, utilize the same time points for the estimation of k values in baseline and in exercise studies. Therefore, the mean transit time approach is more convenient and can provide more objective estimates.

The shape of the myocardial tissue time-activity curves can vary depending on the tracer administration schedule and the shape of the arterial input functions. Values for k_{mono} estimated by the monoexponential fitting approach could be affected by the injection rate of tracer employed even though myocardial oxygen consumption remains constant. The shape of the input function would affect the mean transit time only through an addition of a delay. The values for k estimated by the mean transit time equation in this study are corrected for input function delay and, accordingly, are rather insensitive to the shape of the input function.

Parametric images of biological processes have been shown to facilitate quantitative analysis in the clinical environment (24,26). Because of the computational simplicity of monoexponential fitting, pixel-by-pixel parametric images of k_{mono} values can be easily generated. However, because of the noise sensitivity of monoexponential fitting, heavy smoothing of the dynamic image set (12,13), either by digital filtering or by averaging over a certain number of pixels, is required. Parametric images generated by the method using the mean transit time equation revealed less noisy images than those by monoexponential fitting (Fig. 4). The clinical impact of the noise improvement in the generated parametric images was not examined in this study and remains to be investigated.

The k_{mono} values estimated by monoexponential fitting are not affected by the time-invariant partial volume effect. This is also true for the estimations of k by the mean transit time equation because the equation is normalized by the area of the tissue time-activity curve (Equation 1).

The spillover of radioactivity from the left ventricular chamber to the myocardium is a possible source of error in measuring true myocardial radioactivity concentration. The effects of the spillover correction on the estimated k_{mono} and k values are different for each analytical method. Spillover correction increased the k_{mono} values estimated by monoexponential fitting because the spillover from the left ventricular chamber to the myocardium constitutes a larger fraction of the myocardium curve at later scan times. On the other hand, spillover correction increased mean transit time estimates (Equation 1) because the normalized first moment of the blood-pool time-activity curve is smaller than that of the myocardium time-activity curve and consequently decreased k values estimated by the

mean transit time equation. However, the correction with a spillover fraction of 0.15 did not affect the estimates of k and k_{mono} by more than 5%.

CONCLUSION

The clearance rate constant of the initial phase of the myocardial ^{11}C radioactivity time-activity curve can be estimated using the mean transit time equation. The rate constants estimated with the mean transit time method demonstrated an excellent correlation with the values estimated by conventional monoexponential fitting over a wide range of myocardial oxygen consumption rates. In addition, the estimates obtained noninvasively with ^{11}C -acetate and PET showed a good correlation with the rate pressure products. This approach facilitates objective quantitative analysis of an index of myocardial oxygen consumption because it takes into account the input function delay and because it is insensitive to the selection of kinetic time points for data analysis. The parametric images of the myocardial oxygen consumption index generated by the mean transit time equation also reduced noise. The quality and noise level of the parametric images generated by the mean transit time equation are an improvement over those generated by monoexponential fitting.

ACKNOWLEDGMENTS

The authors thank Ron Sumida, Larry Pang, Francine Aguilar, N. Satyamurthy, PhD and Eileen Rosenfeld for their help in performing this project. This work was supported in part by the Director of the Office of Energy Research, Office of Health and Environmental Research and by research grants #HL 29845, #HL 33177 and #HL 36232 from the National Institutes of Health.

REFERENCES

1. Chan SY, Brunken RC, Phelps ME, Schelbert HR. Use of the metabolic tracer carbon-11-acetate for evaluation of regional myocardial perfusion. *J Nucl Med* 1991;32:665-672.
2. Ng C, Huang SC, Schelbert HR, Buxton DB. A kinetic model for ^{11}C -acetate as a tracer for myocardial oxidative metabolism [Abstract]. *J Nucl Med* 1990;31:1581.
3. Lear JL. Relationship between myocardial clearance rates of carbon-11-acetate-derived radiolabeled and oxidative metabolism: physiologic basis and clinical significance. *J Nucl Med* 1991;32:1957-1960.
4. Brown M, Marshall DR, Sobel BE, Bergmann SR. Delineation of myocardial oxygen utilization with carbon-11-labeled acetate. *Circulation* 1987;76:687-696.
5. Brown MA, Myears DW, Bergmann SR. Noninvasive assessment of canine myocardial oxidative metabolism with carbon-11-acetate and positron emission tomography. *J Am Coll Cardiol* 1988;12:1054-1063.
6. Brown MA, Myears DW, Bergmann SR. Validity of estimates of myocardial oxidative metabolism with carbon-11 acetate and positron emission tomography despite altered patterns of substrate utilization. *J Nucl Med* 1989;30:187-193.
7. Buxton DB, Schwaiger M, Nguyen A, Phelps ME, Schelbert HR. Radiolabeled acetate as a tracer of myocardial tricarboxylic acid cycle flux. *Circ Res* 1988;63:628-634.
8. Buxton DB, Nienaber CA, Luxen A, et al. Noninvasive quantitation of regional myocardial oxygen consumption in vivo with [^{11}C] acetate and dynamic positron emission tomography. *Circulation* 1989;79:134-142.
9. Armbrrecht JJ, Buxton DB, Schelbert HR. Validation of [^{11}C] acetate as a tracer for noninvasive assessment of oxidative metabolism with positron

- emission tomography in normal, ischemic, postischemic and hyperemic canine myocardium. *Circulation* 1990;81:1594-1605.
10. Armbrecht JJ, Buxton DB, Brunken RC, Phelps ME, Schelbert HR. Regional myocardial oxygen consumption determined noninvasively in humans with [^{11}C] acetate and dynamic positron emission tomography. *Circulation* 1989;80:863-872.
 11. Henes CG, Bergmann SR, Walsh MN, Sobel BE, Geltman EM. Assessment of myocardial oxidative metabolic reserve with positron emission tomography and carbon-11-acetate. *J Nucl Med* 1989;30:1489-1499.
 12. Miller TR, Wallis JW, Geltman EM, Bergmann SR. Three-dimensional functional images of myocardial oxygen consumption from positron tomography. *J Nucl Med* 1990;31:2064-2068.
 13. Kotzerke J, Hicks RJ, Wolfe E, et al. Three-dimensional assessment of myocardial oxidative metabolism: a new approach for regional determination of PET-derived carbon-11-acetate kinetics. *J Nucl Med* 1990;31:2064-2068.
 14. Buck A, Wolpers HG, Hutchins GD, et al. Effect of carbon-11-acetate recirculation on estimates of myocardial oxygen consumption by PET. *J Nucl Med* 1991;32:1950-1957.
 15. Lassen NA, Perl W. *Tracer kinetic methods in medical physiology*. New York: Raven Press; 1979:62-101.
 16. Yamaoka K, Nakagawa T, Uno T. Statistical moments in pharmacokinetics. *J Pharmacokinet Biopharm* 1978;6:547-558.
 17. Gillespie WR, Veng-Peterson P. The determination of mean residence time using statistical moments: it is correct. *J Pharmacokinet Biopharm* 1985; 13:549-554.
 18. Kasuya Y, Hirayama H, Kubota N, Pang KS. Interpretation and estimates of mean residence time with statistical theory. *Biopharm Drug Disp* 1987; 8:223-234.
 19. Krivokapich J, Huang SC, Schelbert HR. Assessment of the effects of dobutamine on myocardial blood flow and oxidative metabolism in normal human subjects using ^{13}N ammonia and ^{11}C -acetate: ^{11}C -acetate as a tracer of metabolism and flow. *Am J Cardiol* 1993: in press.
 20. Hoffman EJ, Phelps ME, Huang SC, et al. Dynamic, gated and high resolution imaging with the ECAT III. *IEEE Trans Nucl Sci* 1986;33:452.
 21. Weinberg IN, Huang SC, Hoffman EJ, et al. Validation of PET-acquired input functions for cardiac studies. *J Nucl Med* 1988;29:241-247.
 22. Gambhir SS, Schwaiger M, Huang SC, et al. Simple noninvasive quantification method for measuring myocardial glucose utilization in humans employing positron emission tomography and fluorine-18-deoxyglucose. *J Nucl Med* 1989;30:356-366.
 23. Kuhle W, Porenta G, Buxton D, et al. Quantification of regional myocardial blood flow using ^{13}N ammonia and reoriented dynamic positron emission tomographic imaging. *Circulation* 1992;86:1004-1017.
 24. Choi Y, Hawkins RA, Huang SC, et al. Parametric images of myocardial metabolic rate of glucose generated from dynamic cardiac positron emission tomography and 2- ^{18}F fluoro-2-deoxy-D-glucose studies. *J Nucl Med* 1991; 32:733-738.
 25. Carson RE, Huang SC, Phelps ME. *BLD, a software system for physiological data handling and data analysis*. In: *Proceedings of the fifth annual symposium on computer applications in medical care*. New York: IEEE; 1981:562-565.
 26. Choi Y, Huang SC, Hawkins RA, et al. A simplified method for quantification of myocardial blood flow using ^{13}N -ammonia and dynamic PET. *J Nucl Med* 1993;34:488-497.